

1
2 **Pervasive foreshock activity across southern California**

3
4 **Daniel T. Trugman¹, Zachary E. Ross²**

5 ¹ Geophysics Group, Earth and Environmental Sciences Division, Los Alamos National
6 Laboratory, Los Alamos NM

7 ²Seismological Laboratory, California Institute of Technology, Pasadena CA

8 Corresponding author: Daniel Trugman (dtrugman@lanl.gov)

9
10 **Key Points:**

- 11 • We analyze foreshock activity in a catalog of more than 1.8 million earthquakes in
12 southern California.
- 13 • Foreshock occurrence significantly exceeds the background seismicity rate for 70% of
14 candidate mainshocks.
- 15 • Durations of elevated foreshock activity range from days to weeks for these sequences.

16
17 **DISCLAIMER:** This a non-peer reviewed preprint submitted to EarthArXiv, and is currently
18 under review in the journal *Geophysical Research Letters*.

19
20

21 **Abstract**

22 Foreshocks have been documented as preceding less than half of all mainshock
23 earthquakes. These observations are difficult to reconcile with laboratory earthquake
24 experiments and theoretical models of earthquake nucleation, which both suggest that foreshock
25 activity should be nearly ubiquitous. Here we use a state-of-the-art, high-resolution earthquake
26 catalog to study foreshock sequences of magnitude M4 and greater mainshocks in southern
27 California from 2008-2017. This highly complete catalog provides a new opportunity to examine
28 smaller magnitude precursory seismicity. Seventy percent of mainshocks within this catalog are
29 preceded by foreshock activity that is significantly elevated compared to the local background
30 seismicity rate. Foreshock sequences vary in duration from several days to weeks, with a median
31 of 16.6 days. The results suggest that foreshock occurrence in nature is more prevalent than
32 previously thought, and that our understanding of earthquake nucleation may improve in tandem
33 with advances in our ability to detect small earthquakes.

34 **Plain Language Summary**

35 Earthquakes often occur without warning or detectable precursors. Here we use a new,
36 highly complete earthquake catalog to show that most mainshock earthquakes in southern
37 California are preceded by elevated seismicity rates – foreshocks – in the days and weeks leading
38 up to the event. Many of these foreshock earthquakes are small in magnitude and were hence
39 previously undetected by the seismic network. These observations help bridge the gap between
40 observations of real earth fault systems and laboratory earthquake experiments, where foreshock
41 occurrence is commonly observed.

42 **1 Introduction**

43 There has long been an underlying tension between two competing observations of
44 earthquake occurrence. From one perspective, the occurrence of large earthquakes within a fault
45 zone appears random in time, and indeed classical models of earthquake hazard are based on a
46 Poisson process that encodes this random, memoryless behavior by assumption (Baker, 2013). In
47 contrast, one of the most striking characteristics of earthquakes is that they tend to cluster in
48 space and time, with the triggering of aftershocks following larger, mainshock earthquakes being
49 the best-studied example. The physical mechanisms driving aftershock occurrence are

50 reasonably well-understood, at least a high level: slip on the mainshock fault interface imparts
51 both static (King et al., 1994; Lin & Stein, 2004; Stein, 1999) and dynamic (Brodsky, 2006;
52 Gomberg & Davis, 1996; Kilb et al., 2000; Velasco et al., 2008) stress changes in Earth's crust
53 that trigger aftershock activity. Postseismic fault slip, subcrustal viscoelastic relaxation, and
54 poroelastic stress transfer may also play an important role in certain circumstances (Freed, 2005;
55 Freed & Lin, 2001; Koper et al., 2018; Ross et al., 2017).

56 Foreshocks – earthquake occurrences preceding mainshocks – are less well understood.
57 While it is unambiguous that foreshocks do occasionally occur, both their physical significance
58 and their relative prevalence are subject to vigorous debate (Ellsworth & Bulut, 2018; Seif et al.,
59 2019; Shearer & Lin, 2009; Tape et al., 2018). In laboratory earthquake experiments, precursory
60 slip events analogous to foreshocks are observed in nearly all instances (Bolton et al., 2019;
61 Johnson et al., 2013; Rouet-Leduc et al., 2017; W. Goebel et al., 2013). Likewise, theoretical
62 models of fault friction, including the widely used rate-and-state framework, typically require a
63 seismic nucleation phase preceding dynamic rupture (Ampuero & Rubin, 2008; Dieterich, 1994;
64 Marone, 1998). These facets of laboratory and theoretical earthquake behavior suggest that
65 foreshock occurrence may be a natural manifestation of a nucleation or preslip process preceding
66 rupture (Bouchon et al., 2013; Dodge et al., 1996). This interpretation if correct would have
67 important scientific and practical consequences, and would intimate that foreshocks could
68 potentially be used to forecast characteristics of eventual mainshock occurrence.

69 One problem with this interpretation is that foreshock activity in nature is not observed as
70 frequently as it should be if it were a universal feature of earthquake nucleation. While it is
71 notoriously difficult to compare different foreshock studies due to different magnitude thresholds
72 or space-time selection windows (Reasenber, 1999), foreshocks have previously been observed
73 to precede 10-50% of mainshocks (Abercrombie & Mori, 1996; Chen & Shearer, 2016; Jones &
74 Molnar, 1976; Marsan et al., 2014; Reasenber, 1999). Taking these observations at face value,
75 what happens during the nucleation process of the other 50 to 90% of earthquakes? Are there
76 really no foreshocks, or are we simply not listening closely enough to detect them? The notion
77 that there exists undetected but substantial foreshock activity is supported by a recent meta-
78 analysis of 37 different studies of foreshocks (Mignan, 2014), which revealed systematic
79 differences in the outcome depending on the minimum magnitude of foreshock detected. A
80 similar effect can be seen in laboratory experiments, as the ability to forecast imminent

81 laboratory earthquakes depends fundamentally on the magnitude of completion of precursory
82 slip events (Lubbers et al., 2018).

83 In this study, we measure foreshock activity using a powerful new tool: a state-of-the-art
84 earthquake catalog (Ross et al., 2019) of more than 1.81 million earthquakes that occurred in
85 southern California from 2008 through 2017. The extraordinary detail of this catalog, which is
86 complete regionally down to M0.3 and locally down M0.0 or less, allows us to examine
87 precursory seismicity at the smallest of scales, in direct analog to well-recorded laboratory
88 experiments. We find that elevated foreshock activity is pervasive in southern California, with
89 70% of earthquake sequences exhibiting a significant, local increase in seismicity rate preceding
90 the mainshock event. The spatiotemporal evolution of these sequences is diverse in character, a
91 fact which may preclude real-time forecasting based on foreshock activity. Nevertheless, these
92 results help bridge the gap in our understanding of precursory activity from laboratory to Earth
93 scales.

94 **2 Earthquake Catalog Data**

95 We analyze earthquake sequences in southern California derived from the Quake
96 Template Matching (QTM) earthquake catalog (Ross et al., 2019). This recently released catalog
97 of southern California seismicity from 2008 – 2017 was compiled using approximately 284,000
98 earthquakes listed in the Southern California Seismic Network (SCSN) catalog (Hutton et al.,
99 2010) as templates for network-wide waveform cross-correlation (Gibbons & Ringdal, 2006;
100 Shelly et al., 2007), yielding more than 1.81 million detected earthquakes. The vast majority of
101 these newly detected earthquakes are small in magnitude ($-2 < M < 0$), well beneath the M1.7
102 completeness threshold of the original SCSN catalog. The QTM catalog, by contrast, is more
103 than an order of magnitude more complete, with consistent detection at M0.0 and below in
104 regions of dense station coverage.

105 We examine foreshock activity for magnitude M4 and greater mainshocks located within
106 the latitude and longitude ranges of $[32.68^\circ, 36.20^\circ]$ and $[-118.80^\circ, -115.40^\circ]$. This spatial
107 boundary was guided by the density of the SCSN station coverage and the local magnitude of
108 completeness (Figure S1), since in more remote locations the template matching detection

109 threshold is poorer. The lower latitude boundary of 32.68° is set to approximate the
 110 California/Mexico border, so the study region only contains events within southern California.

111 Within this study region, we select a total of 43 mainshocks that are relatively isolated in
 112 space and time from other larger events, to ensure that the selected events are indeed mainshocks
 113 as traditionally defined, and that the seismicity rate during the pre-event window is not biased
 114 high due to aftershock triggering from unrelated events. To do this, we use a magnitude-
 115 dependent windowing criterion to exclude events within (i) 40 days and 40 km another M4
 116 event, (ii) 80 km, 80 days of an M5 event, (iii) 160 km, 160 days of an M6 event, or (iv) 240 km,
 117 240 days of an M7 event. We note that this criteria removes a large number of potential
 118 mainshocks occurring in the months following the 2010 M7.2 El Mayor-Cucapah earthquake,
 119 when the high triggered seismicity rate (Hauksson et al., 2011; Meng & Peng, 2014) renders
 120 foreshock analyses problematic. The El Mayor-Cucapah event is not considered in this study due
 121 to its location in Baja California, to south of our study region, though it was itself preceded by a
 122 notable foreshock sequence (Chen & Shearer, 2013).

123 **3 Methods**

124 For each selected mainshock, we measure the local background rate of seismicity within
 125 10 km epicentral distance of the mainshock using the interevent time method (Hainzl et al.,
 126 2006). In this technique, the set of observed interevent time differences τ between subsequent
 127 events, are modeled as gamma distribution:

$$128 \quad p(\tau) = C \cdot \tau^{\gamma-1} \cdot e^{-\mu \tau}. \quad (1)$$

129 Here, μ is the background rate, γ is the fraction of the total events that are background
 130 events, and $C = \mu^\gamma / \Gamma(\gamma)$ is a normalizing constant. The appeal of the interevent time method is
 131 that it can be used to extract a background rate from temporally clustered earthquake catalog data
 132 without assuming an explicit functional form for triggered, non-background seismicity as in the
 133 popular epidemic type aftershock sequence (ETAS) model (Ogata, 1988). For each earthquake,

134 we solve for μ using a maximum likelihood approach (van Stiphout et al., 2012), and estimate
135 uncertainties using a log-transformed jackknife procedure (Efron & Stein, 1981).

136 Having established the local background rate, we consider potential foreshocks within
137 this same 10 km distance range from the mainshock. While most previous studies neglect the
138 local background rate and consider any earthquake sufficiently close in space and time to the
139 mainshock to be a foreshock (Abercrombie & Mori, 1996; Chen & Shearer, 2016), this
140 assumption is clearly problematic for the QTM catalog due to its high spatiotemporal event
141 density. Thus, to measure the statistical significance of foreshock activity, we count the observed
142 number of earthquakes N in the 20 days preceding the mainshock, and use Monte Carlo
143 simulations to compute the probability p of observing at least N events during the 20-day / 10-km
144 window, given the background rate μ and its uncertainty. Low p -values are indicative of
145 foreshock activity rates in excess of the background rate, and we consider $p < 0.01$ to be
146 statistically significant evidence for elevated foreshock activity.

147 These background rate estimates, when combined with the relative completeness of the
148 QTM catalog, enable measurement of the duration of significant foreshock activity, a subject that
149 has not been carefully studied to date. To do this, we calculate the event rate within 5-day
150 moving windows (and the same 10 km spatial windows). We work backwards in time from the
151 mainshock origin time $T = 0$, in steps of 0.1 days, until the observed event rate falls to within
152 one standard deviation of the background rate μ , and take the window end time to be the
153 duration estimate. We use a 5-day window (rather than, for example, 10 days or 20 days), as we
154 found it to be the best compromise between precision in defining the onset of foreshock
155 sequences, and robustness to short-duration gaps in seismicity. Measurement uncertainties in the
156 duration estimates are of order 1 day, controlled primarily by the uncertainty in the background
157 rate and the temporal averaging (5 days) used to compute the observed event rates.

158 It is also important to understand how improved catalog completeness augments our
159 understanding of foreshock sequences. This issue is pertinent both within and beyond the study
160 region of California, as future studies in regions across the globe will provide new high-
161 resolution catalogs by applying advanced event detection techniques (Kong et al., 2019; Yoon et
162 al., 2015). To address this question in southern California, we repeat our analysis of the 43

163 foreshock sequences using the SCSN catalog instead of the QTM catalog, using an identical
164 procedure to calculate background rates and compute the p -value of the observed foreshock
165 count within 20 days and 10 km (Figure S2).

166 **4 Results**

167 In total, 30 out of 43 mainshocks in southern California have a statistically significant
168 increase in foreshock activity relative to the background seismicity rate (Figure 1 and Table S1).
169 This 70% fraction suggests that precursory seismicity is more ubiquitous than previously
170 understood, and that the discrepancy between the prevalence of foreshocks in laboratory and real
171 Earth studies may in part be explained by observation limitations. This hypothesis is supported
172 through direct comparison with the SCSN catalog, in which only 21 of the 43 sequences exhibit
173 significant foreshock activity. This fraction is consistent with recent studies of foreshocks in
174 California (Chen & Shearer, 2016), which helps validate our methodology.

175 The improvement in the resolution of foreshock sequences using the QTM catalog is
176 particularly notable given that the SCSN catalog with a nominal magnitude of completeness of
177 M1.7, is among the highest quality network-based catalogs currently available. Despite this,
178 there are numerous cases in which the SCSN catalog misses foreshock sequences entirely
179 (Figures 2 and 3). In other instances where foreshock activity is apparent in both catalogs, the
180 QTM catalog provides improved detail of the low-magnitude foreshock events that provide a
181 more complete perspective of the nucleation process. For example, in the earthquake sequences
182 depicted in Figure 4, the precise timing of the onset of each foreshock sequence is readily
183 apparent using the QTM catalog, but is impossible to discern using the SCSN catalog alone.

184 The QTM catalog also provides a unique opportunity to examine the spatial and temporal
185 characteristics of foreshock sequences in southern California. We can, for example, estimate the
186 duration of foreshock activity by measuring the timespan preceding the mainshock for which the
187 pre-event seismicity rate significantly exceeds the background rate (Figures 2-4, see Methods).
188 Estimated foreshock durations for the 30 sequences range in length from 3 to 35 days, with a
189 median of 16.6 days (Table S1). The duration estimates are limited in their precision by the
190 uncertainty in the background rate and the temporal averaging required to compute the observed

191 event rate. However, with nominal uncertainties of order 1 day, they still provide a useful
192 measure of the temporal extent of elevated foreshock activity.

193 The foreshock sequences are diverse in their spatiotemporal evolution. Many of the
194 longer-duration sequences are earthquake swarms that have been previously documented in
195 select regions of southern California (Zhang & Shearer, 2016). A number of mainshocks are
196 preceded by burst-like foreshock sequences near the mainshock hypocenter in the days and hours
197 leading up to the event, while still others have a more diffuse and widespread elevation in
198 seismicity rate (Figure 4 and Figure S3). Likewise, there are some notable instances of
199 systematic linear migration in foreshocks toward the mainshock hypocenter, but this behavior is
200 not universally observed. Indeed, these sequences exemplify the diverse characteristics one
201 might anticipate in complex natural fault systems.

202 We do not observe variations in foreshock behavior related to mainshock magnitude or
203 focal mechanism type, and the slight trend for shallow mainshocks to have more intense
204 foreshock activity is not statistically significant given our relatively small sample size of
205 candidate mainshocks (Figure S4). These findings may in part be attributed to the relative
206 homogeneity in tectonic regime of the study region of southern California (Reasenber, 1999).
207 There are, however, subtle regional differences in foreshock activity. For example, the
208 earthquake sequences nearest the Salton Sea and Coso geothermal field all feature extensive
209 foreshock activity, while several well-recorded sequences near coastal Los Angeles do not
210 (Figure 1). We note that at least two of the sequences without significant foreshock activity are
211 within a remote part of the Eastern California Shear Zone with relatively sparse station coverage,
212 so it is possible that smaller magnitude foreshocks in those particular sequences went undetected.
213 Further, our significance criterion of $p < 0.01$ is conservative by design, and thus selects only the
214 most robustly observed foreshock sequences. There are six additional sequences with $0.01 < p <$
215 0.1 in which the observed seismicity rates exceed the inferred background rate, but not to the
216 extent where the physical significance of this rate increase is unambiguous.

217 **5 Conclusions**

218 We use a detailed new earthquake catalog to demonstrate that elevated foreshock activity
219 is much more common than previously understood. The details of these foreshock sequences

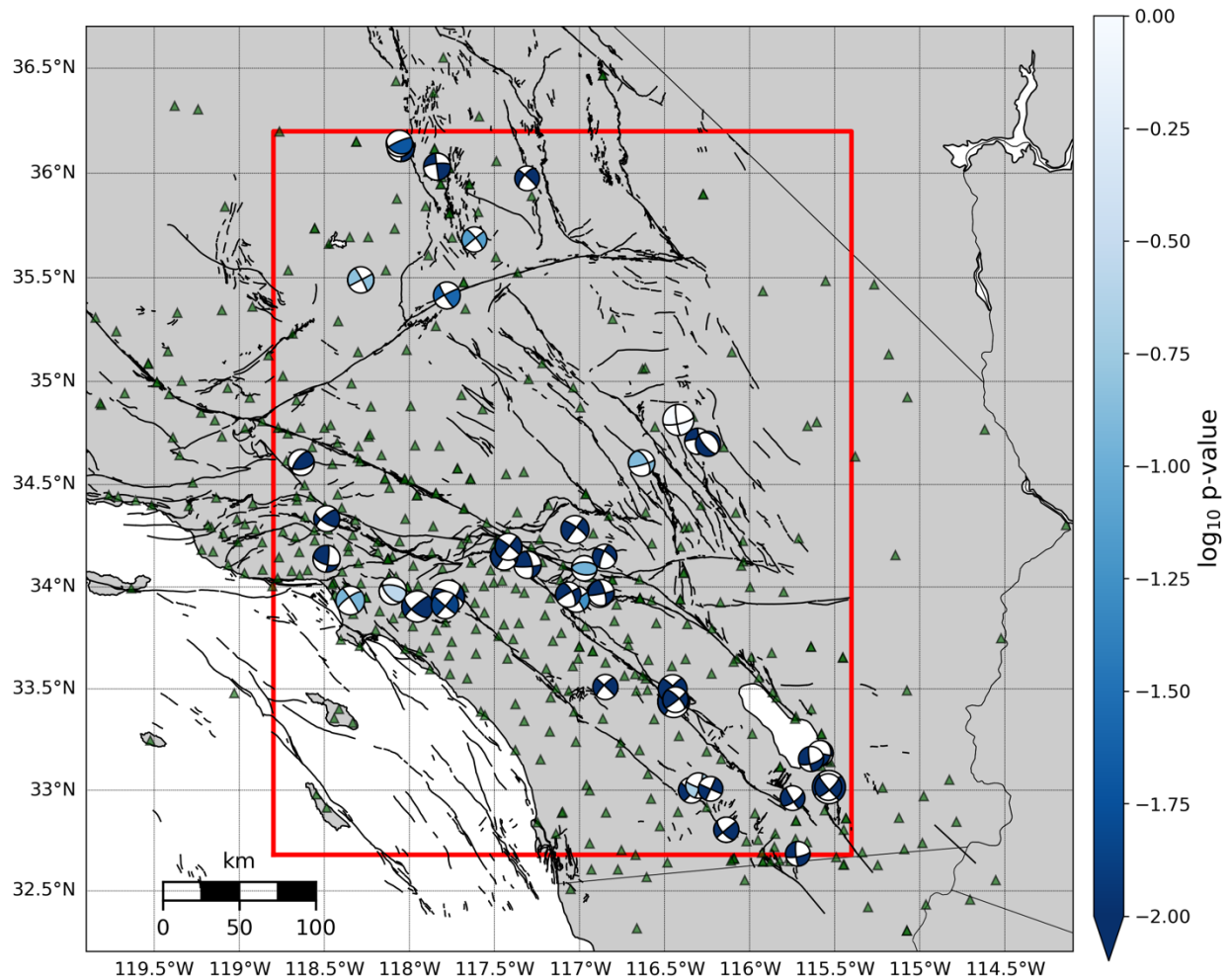
220 have to date been obscured by limitations in catalog completeness, even in southern California,
221 where the SCSN maintains one of the most complete regional earthquake catalogs in the world.
222 The prevalence of measurable foreshock activity we observe is reminiscent of laboratory
223 experiments, where low-amplitude precursory slip events are ubiquitously observed preceding
224 failure. In the laboratory, the statistical characteristics of these slip events can be used to predict
225 the properties of imminent mainshocks, including their timing and slip amplitudes (Hulbert et al.,
226 2019; Rouet-Leduc et al., 2017).

227 Despite the notable similarities with laboratory studies, the complexity observed in the
228 real Earth will likely preclude hazard monitoring based on foreshock activity for the foreseeable
229 future. Even within the limited study region of southern California, foreshock sequences vary
230 substantially in duration and spatiotemporal evolution. Likewise, in real fault systems,
231 precursory activity is not a unique cause of elevated seismicity rates, which are more commonly
232 observed in association with aftershock triggering. While foreshock activity may be apparent in
233 retrospect after careful statistical analyses, identifying foreshocks in real time presents a whole
234 new set of challenges that we do not attempt to address in this work. It is also important to note
235 that there are several instances of well-recorded mainshock events within our catalog that occur
236 without detectable foreshocks, a fact which suggests that the nucleation processes of individual
237 earthquakes are diverse rather than universal in character. Nevertheless, by examining the details
238 of earthquake activity at the finest of scales, we will improve our understanding of the physical
239 mechanisms underlying how earthquakes get started.

240 **Acknowledgments**

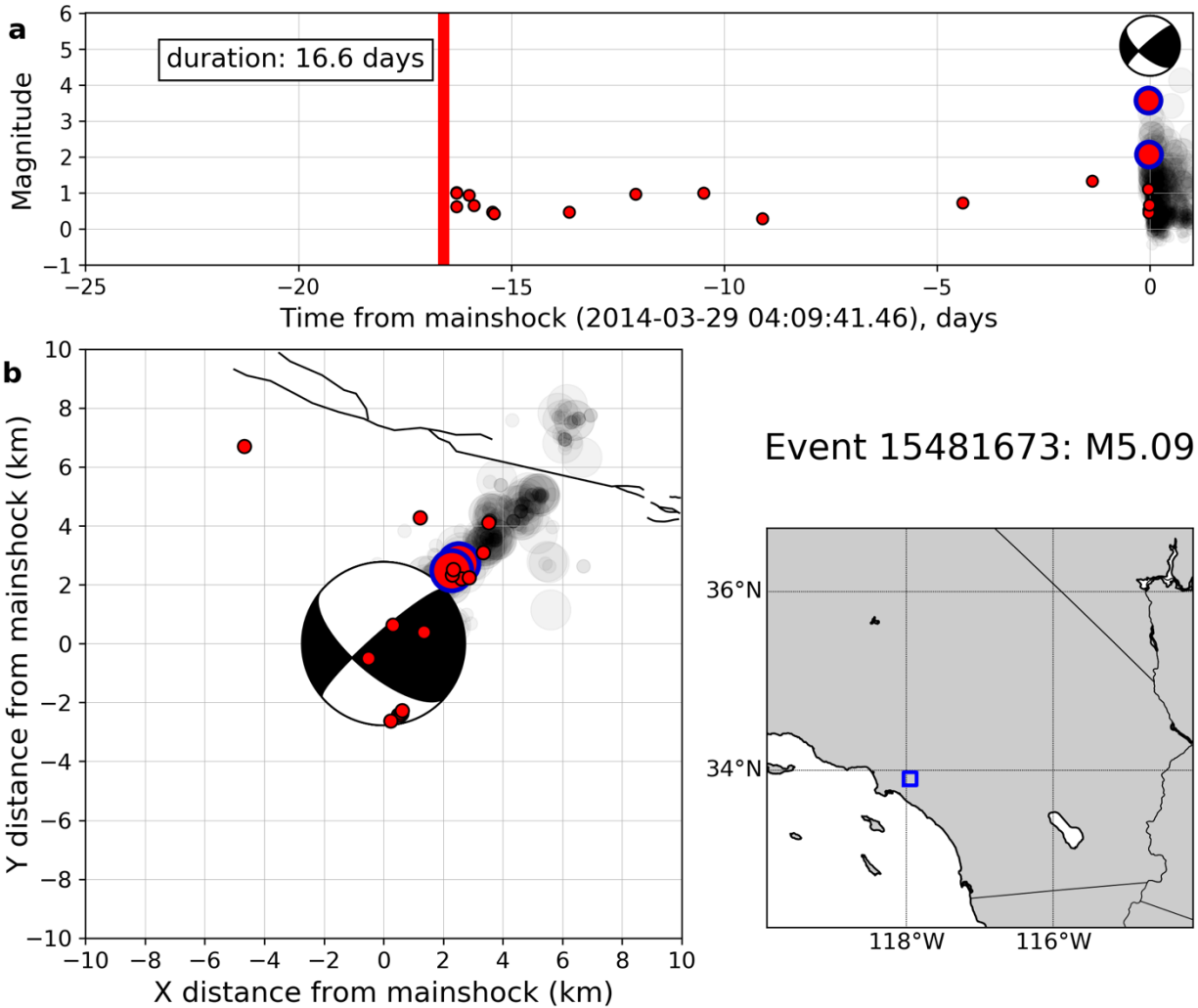
241 The two earthquake catalogs analyzed in the manuscript are publicly available online.
242 The QTM catalog and the SCSN catalog are both archived by the Southern California
243 Earthquake Data Center (scedc.caltech.edu/). The workflow and statistical analysis described in
244 the Methods section was performed using open source python software packages. D. Trugman
245 acknowledges institutional support from the Laboratory Directed Research and Development
246 (LDRD) program of Los Alamos National Laboratory under project number 20180700PRD1.
247 We are grateful to P. Johnson, I. McBrearty, and N. Lubbers for their helpful advice that
248 improved the manuscript.

249

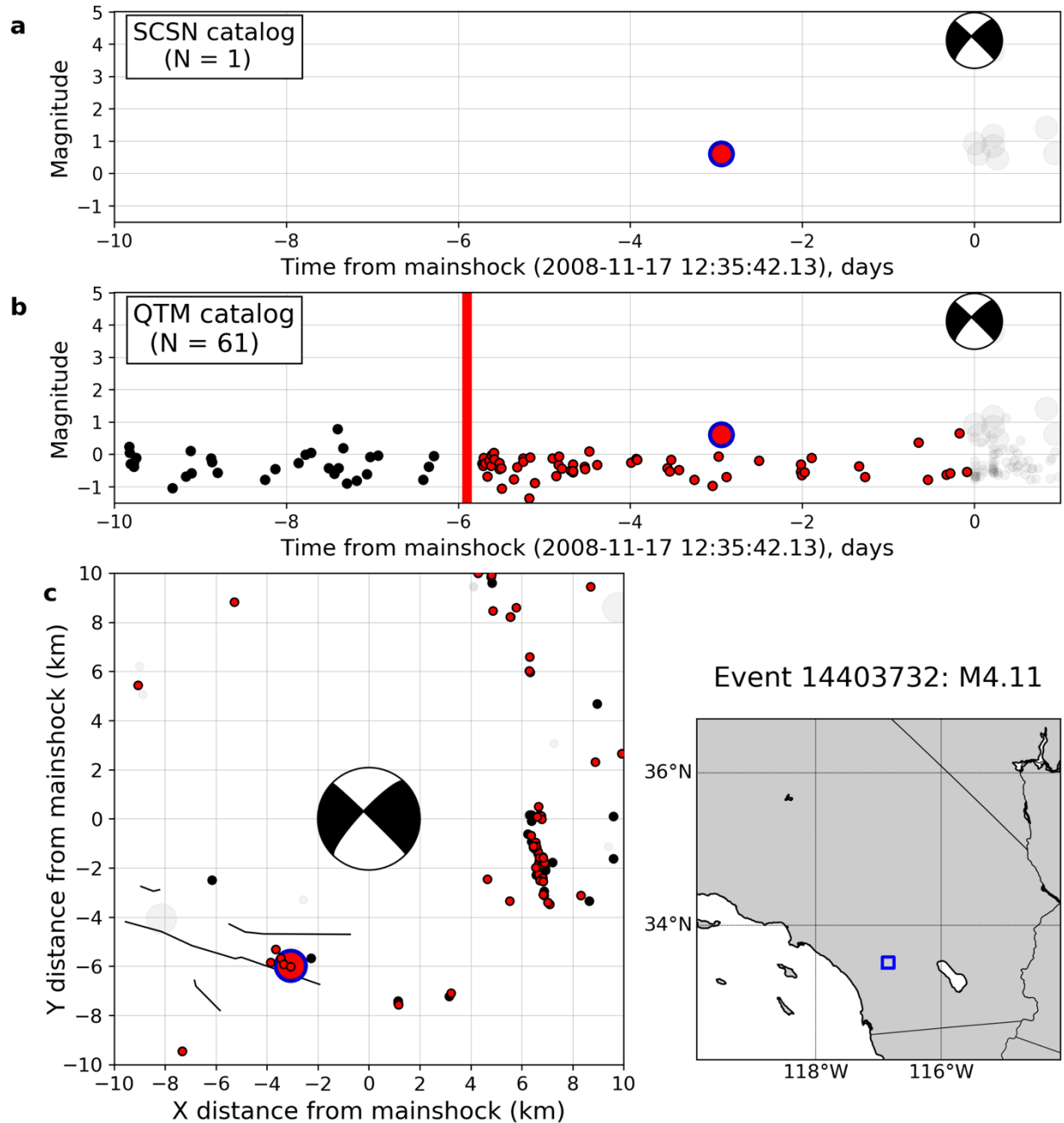


250

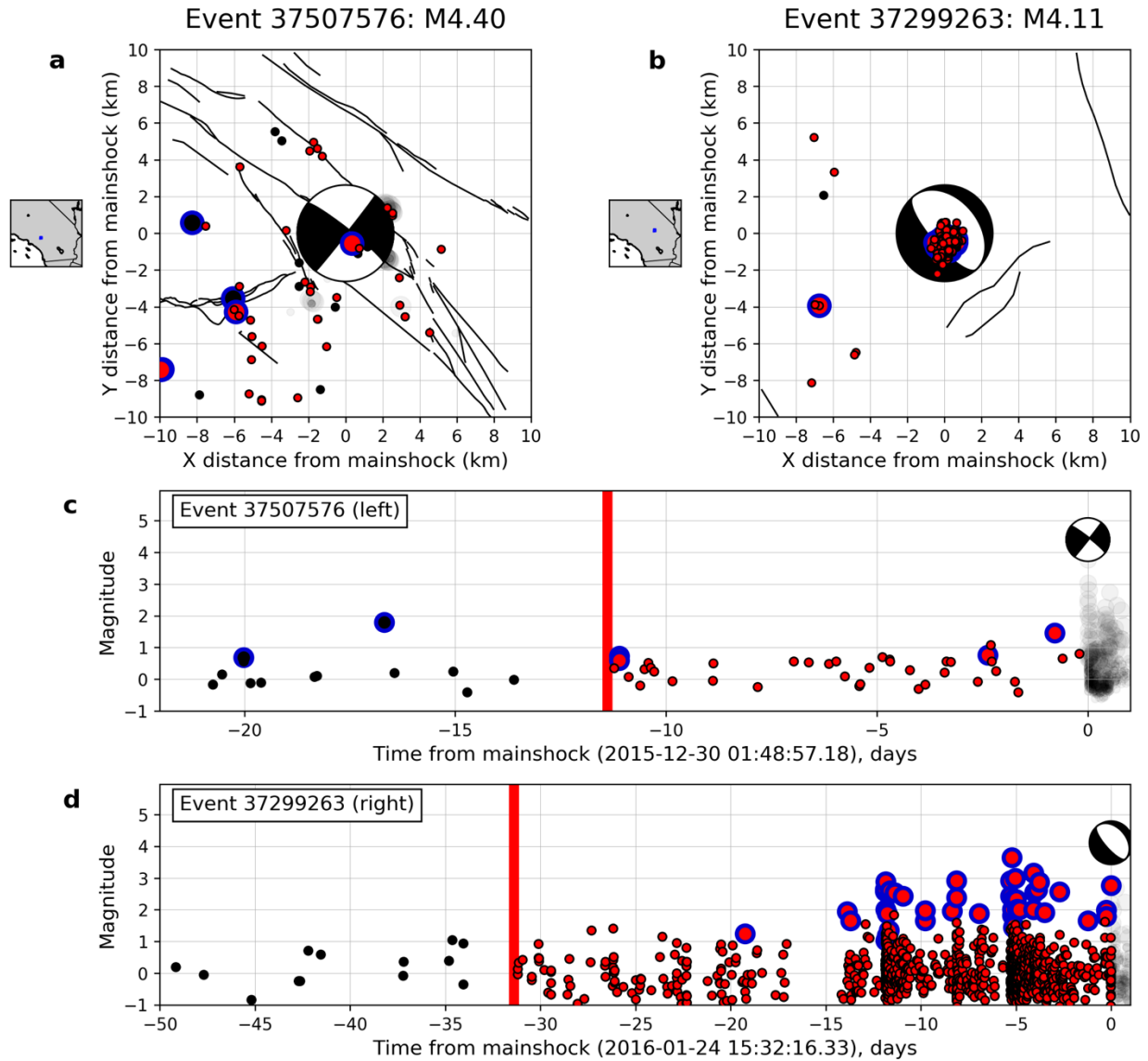
251 **Figure 1.** Foreshock sequences of 43 M4 and M5 earthquakes in southern California. The study
 252 region outlined in red – $[32.68^\circ, 36.20^\circ]$ latitude and $[-118.80^\circ, -115.40^\circ]$ longitude – was
 253 selected to ensure a sufficiently low magnitude of completion for detection (Figure S1). Each
 254 event is color-coded by the p -value measurement of foreshock activity described in the text, with
 255 lower p -values (darker colors) indicating more significant activity.



256
 257 **Figure 2.** Example foreshock sequence for a M5.09 earthquake occurring during January 2016
 258 (Event 15481673). (a) Earthquake magnitude versus time for events within a 10km region of the
 259 mainshock. Large circles with solid blue lines denote events listed within the SCSN catalog,
 260 while small circles denote newly detected events listed by the QTM catalog. The inferred
 261 foreshock duration of 16.6 days is denoted with a vertical red line. (b) Map view of the foreshock
 262 sequence and its location within southern California.



263
 264 **Figure 3.** Hidden foreshocks revealed by the improved detection capability of the QTM catalog.
 265 Panels (a) and (b) compare the magnitude-time evolution of the foreshock sequence for an
 266 example earthquake (Event 14403732) from the perspective of (a) the SCSN catalog (b) the
 267 QTM catalog. In the 6 days preceding this event, only one SCSN earthquake was recorded,
 268 compared to 61 in the QTM catalog. Red circles denote events following the estimated foreshock
 269 duration (red line), while black circles denote events preceding this. (c) Map view of the
 270 foreshock sequence and its location within southern California.



271
 272 **Figure 4.** Diverse patterns of foreshock occurrence in southern California. Panels (a) and (b)
 273 show map view representations of two distinct foreshock sequences, one (a) with an extended
 274 period of elevated seismicity rate surrounding the mainshock hypocenter, and the other (b) with
 275 several highly localized bursts of seismicity preceding the mainshock. Red circles denote events
 276 following the estimated foreshock duration (red line), while black circles denote events
 277 preceding this. Large circles with solid blue lines denote events listed within the SCSN catalog,
 278 while small circles denote newly detected events listed by the QTM catalog. (c) and (d) Event
 279 magnitude versus time for the sequences shown in panels a and b, respectively.
 280

281 **References**

- 282 Abercrombie, R. E., & Mori, J. (1996). Occurrence patterns of foreshocks to large earthquakes in
283 the western United States. *Nature*, *381*(6580), 303–307.
284 <https://doi.org/10.1038/381303a0>
- 285 Ampuero, J.-P., & Rubin, A. M. (2008). Earthquake nucleation on rate and state faults - Aging
286 and slip laws. *Journal of Geophysical Research*, *113*(B1).
287 <https://doi.org/10.1029/2007JB005082>
- 288 Baker, J. W. (2013). An introduction to probabilistic seismic hazard analysis. *White Paper*
289 *Version 2.0*, 1–79.
- 290 Bolton, D. C., Shokouhi, P., Rouet-Leduc, B., Hulbert, C., Rivière, J., Marone, C., & Johnson, P.
291 A. (2019). Characterizing Acoustic Signals and Searching for Precursors during the
292 Laboratory Seismic Cycle Using Unsupervised Machine Learning. *Seismological*
293 *Research Letters*, *90*(3), 1088–1098. <https://doi.org/10.1785/0220180367>
- 294 Bouchon, M., Durand, V., Marsan, D., Karabulut, H., & Schmittbuhl, J. (2013). The long
295 precursory phase of most large interplate earthquakes. *Nature Geoscience*, *6*(4), 299–302.
296 <https://doi.org/10.1038/ngeo1770>
- 297 Brodsky, E. E. (2006). Long-range triggered earthquakes that continue after the wave train
298 passes. *Geophysical Research Letters*, *33*(15). <https://doi.org/10.1029/2006GL026605>
- 299 Chen, X., & Shearer, P. M. (2013). California foreshock sequences suggest aseismic triggering
300 process. *Geophysical Research Letters*, *40*(11), 2602–2607.
301 <https://doi.org/10.1002/grl.50444>
- 302 Chen, X., & Shearer, P. M. (2016). Analysis of Foreshock Sequences in California and
303 Implications for Earthquake Triggering. *Pure and Applied Geophysics*, *173*(1), 133–152.
304 <https://doi.org/10.1007/s00024-015-1103-0>

- 305 Dieterich, J. (1994). A constitutive law for rate of earthquake production and its application to
306 earthquake clustering. *Journal of Geophysical Research*, 99(B2), 2601.
307 <https://doi.org/10.1029/93JB02581>
- 308 Dodge, D. A., Beroza, G. C., & Ellsworth, W. L. (1996). Detailed observations of California
309 foreshock sequences: Implications for the earthquake initiation process. *Journal of*
310 *Geophysical Research: Solid Earth*, 101(B10), 22371–22392.
311 <https://doi.org/10.1029/96JB02269>
- 312 Efron, B., & Stein, C. (1981). The Jackknife Estimate of Variance. *The Annals of Statistics*, 9(3),
313 586–596. <https://doi.org/10.1214/aos/1176345462>
- 314 Ellsworth, W. L., & Bulut, F. (2018). Nucleation of the 1999 Izmit earthquake by a triggered
315 cascade of foreshocks. *Nature Geoscience*, 1. <https://doi.org/10.1038/s41561-018-0145-1>
- 316 Freed, A. M. (2005). Earthquake triggering by static, dynamic and postseismic stress transfer.
317 *Annual Review of Earth and Planetary Sciences*, 33(1), 335–367.
318 <https://doi.org/10.1146/annurev.earth.33.092203.122505>
- 319 Freed, A. M., & Lin, J. (2001). Delayed triggering of the 1999 Hector Mine earthquake by
320 viscoelastic stress transfer. *Nature*, 411(6834), 180–183.
321 <https://doi.org/10.1038/35075548>
- 322 Gibbons, S. J., & Ringdal, F. (2006). The detection of low magnitude seismic events using array-
323 based waveform correlation. *Geophysical Journal International*, 165(1), 149–166.
324 <https://doi.org/10.1111/j.1365-246X.2006.02865.x>
- 325 Gomberg, J., & Davis, S. (1996). Stress/strain changes and triggered seismicity at The Geysers,
326 California. *Journal of Geophysical Research*, 101(B1), 733.
327 <https://doi.org/10.1029/95JB03250>

- 328 Hainzl, S., Scherbaum, F., & Beauval, C. (2006). Estimating Background Activity Based on
329 Interevent-Time Distribution. *Bulletin of the Seismological Society of America*, *96*(1),
330 313–320. <https://doi.org/10.1785/0120050053>
- 331 Hauksson, E., Stock, J., Hutton, K., Yang, W., Vidal-Villegas, J., & Kanamori, H. (2011). The
332 2010 Mw 7.2 El Mayor-Cucapah Earthquake Sequence, Baja California, Mexico and
333 Southernmost California, USA: Active Seismotectonics along the Mexican Pacific
334 Margin. *Pure and Applied Geophysics*, *168*(8–9), 1255–1277.
- 335 Hulbert, C., Rouet-Leduc, B., Johnson, P. A., Ren, C. X., Rivière, J., Bolton, D. C., & Marone,
336 C. (2019). Similarity of fast and slow earthquakes illuminated by machine learning.
337 *Nature Geoscience*, *12*(1), 69. <https://doi.org/10.1038/s41561-018-0272-8>
- 338 Hutton, K., Woessner, J., & Hauksson, E. (2010). Earthquake Monitoring in Southern California
339 for Seventy-Seven Years (1932-2008). *Bulletin of the Seismological Society of America*,
340 *100*(2), 423–446. <https://doi.org/10.1785/0120090130>
- 341 Johnson, P. A., Ferdowsi, B., Kaproth, B. M., Scuderi, M., Griffa, M., Carmeliet, J., et al. (2013).
342 Acoustic emission and microslip precursors to stick-slip failure in sheared granular
343 material. *Geophysical Research Letters*, *40*(21), 5627–5631.
344 <https://doi.org/10.1002/2013GL057848>
- 345 Jones, L., & Molnar, P. (1976). Frequency of foreshocks. *Nature*, *262*(5570), 677.
346 <https://doi.org/10.1038/262677a0>
- 347 Kilb, D., Gomberg, J., & Bodin, P. (2000). Triggering of earthquake aftershocks by dynamic
348 stresses. *Nature*, *408*(6812), 570–574. <https://doi.org/10.1038/35046046>
- 349 King, G. C. P., Stein, R. S., & Lin, J. (1994). Static stress changes and the triggering of
350 earthquakes. *Bulletin of the Seismological Society of America*, *84*(3), 935–953.

- 351 Kong, Q., Trugman, D. T., Ross, Z. E., Bianco, M. J., Meade, B. J., & Gerstoft, P. (2019).
352 Machine Learning in Seismology: Turning Data into Insights. *Seismological Research*
353 *Letters*, 90(1), 3–14. <https://doi.org/10.1785/0220180259>
- 354 Koper, K. D., Pankow, K. L., Pechmann, J. C., Hale, J. M., Burlacu, R., Yeck, W. L., et al.
355 (2018). Afterslip Enhanced Aftershock Activity During the 2017 Earthquake Sequence
356 Near Sulphur Peak, Idaho. *Geophysical Research Letters*, 45(11), 5352–5361.
357 <https://doi.org/10.1029/2018GL078196>
- 358 Lin, J., & Stein, R. S. (2004). Stress triggering in thrust and subduction earthquakes and stress
359 interaction between the southern San Andreas and nearby thrust and strike-slip faults.
360 *Journal of Geophysical Research: Solid Earth (1978–2012)*, 109(B2).
- 361 Lubbers, N., Bolton, D. C., Mohd-Yusof, J., Marone, C., Barros, K., & Johnson, P. A. (2018).
362 Earthquake Catalog-Based Machine Learning Identification of Laboratory Fault States
363 and the Effects of Magnitude of Completeness. *Geophysical Research Letters*, 45(24),
364 13,269–13,276. <https://doi.org/10.1029/2018GL079712>
- 365 Marone, C. (1998). Laboratory-Derived Friction Laws and Their Application to Seismic
366 Faulting. *Annual Review of Earth and Planetary Sciences*, 26(1), 643–696.
367 <https://doi.org/10.1146/annurev.earth.26.1.643>
- 368 Marsan, D., Helmstetter, A., Bouchon, M., & Dublanchet, P. (2014). Foreshock activity related
369 to enhanced aftershock production. *Geophysical Research Letters*, 41(19), 6652–6658.
370 <https://doi.org/10.1002/2014GL061219>
- 371 Meng, X., & Peng, Z. (2014). Seismicity rate changes in the Salton Sea Geothermal Field and the
372 San Jacinto Fault Zone after the 2010 Mw 7.2 El Mayor-Cucapah earthquake.

- 373 *Geophysical Journal International*, 197(3), 1750–1762.
374 <https://doi.org/10.1093/gji/ggu085>
- 375 Mignan, A. (2014). The debate on the prognostic value of earthquake foreshocks: A meta-
376 analysis. *Scientific Reports*, 4, 4099. <https://doi.org/10.1038/srep04099>
- 377 Ogata, Y. (1988). Statistical Models for Earthquake Occurrences and Residual Analysis for Point
378 Processes. *Journal of the American Statistical Association*, 83(401), 9–27.
379 <https://doi.org/10.1080/01621459.1988.10478560>
- 380 Reasenber, P. A. (1999). Foreshock occurrence before large earthquakes. *Journal of*
381 *Geophysical Research: Solid Earth*, 104(B3), 4755–4768.
382 <https://doi.org/10.1029/1998JB900089>
- 383 Ross, Z. E., Rollins, C., Cochran, E. S., Hauksson, E., Avouac, J.-P., & Ben-Zion, Y. (2017).
384 Aftershocks driven by afterslip and fluid pressure sweeping through a fault-fracture
385 mesh. *Geophysical Research Letters*, 44(16), 2017GL074634.
386 <https://doi.org/10.1002/2017GL074634>
- 387 Ross, Z. E., Trugman, D. T., Hauksson, E., & Shearer, P. M. (2019). Searching for hidden
388 earthquakes in Southern California. *Science*, eaaw6888.
389 <https://doi.org/10.1126/science.aaw6888>
- 390 Rouet-Leduc, B., Hulbert, C., Lubbers, N., Barros, K., Humphreys, C. J., & Johnson, P. A.
391 (2017). Machine Learning Predicts Laboratory Earthquakes. *Geophysical Research*
392 *Letters*, 44(18), 2017GL074677. <https://doi.org/10.1002/2017GL074677>
- 393 Seif, S., Zechar, J. D., Mignan, A., Nandan, S., & Wiemer, S. (2019). Foreshocks and Their
394 Potential Deviation from General Seismicity. *Bulletin of the Seismological Society of*
395 *America*, 109(1), 1–18. <https://doi.org/10.1785/0120170188>

- 396 Shearer, P. M., & Lin, G. (2009). Evidence for Mogi doughnut behavior in seismicity preceding
397 small earthquakes in southern California. *Journal of Geophysical Research: Solid Earth*,
398 *114*(B1). <https://doi.org/10.1029/2008JB005982>
- 399 Shelly, D. R., Beroza, G. C., & Ide, S. (2007). Non-volcanic tremor and low-frequency
400 earthquake swarms. *Nature*, *446*(7133), 305–307. <https://doi.org/10.1038/nature05666>
- 401 Stein, R. S. (1999). The role of stress transfer in earthquake occurrence. *Nature*, *402*(6762), 605–
402 609. <https://doi.org/10.1038/45144>
- 403 van Stiphout, T., Zhuang, J., & Marsan, D. (2012). Seismicity declustering. *Community Online*
404 *Resource for Statistical Seismicity Analysis*, *10*, 1.
- 405 Tape, C., Holtkamp, S., Silwal, V., Hawthorne, J., Kaneko, Y., Ampuero, J. P., et al. (2018).
406 Earthquake nucleation and fault slip complexity in the lower crust of central Alaska.
407 *Nature Geoscience*, *1*. <https://doi.org/10.1038/s41561-018-0144-2>
- 408 Velasco, A. A., Hernandez, S., Parsons, T., & Pankow, K. (2008). Global ubiquity of dynamic
409 earthquake triggering. *Nature Geoscience*, *1*(6), 375–379.
410 <https://doi.org/10.1038/ngeo204>
- 411 W. Goebel, T. H., Schorlemmer, D., Becker, T. W., Dresen, G., & Sammis, C. G. (2013).
412 Acoustic emissions document stress changes over many seismic cycles in stick-slip
413 experiments. *Geophysical Research Letters*, *40*(10), 2049–2054.
414 <https://doi.org/10.1002/grl.50507>
- 415 Yoon, C. E., O'Reilly, O., Bergen, K. J., & Beroza, G. C. (2015). Earthquake detection through
416 computationally efficient similarity search. *Science Advances*, *1*(11), e1501057.
417 <https://doi.org/10.1126/sciadv.1501057>

418 Zhang, Q., & Shearer, P. M. (2016). A new method to identify earthquake swarms applied to
419 seismicity near the San Jacinto Fault, California. *Geophysical Journal International*,
420 205(2), 995–1005. <https://doi.org/10.1093/gji/ggw073>

421